ISSN: 1410-8917
Jurnal Kimia Sains & Aplikasi
e-ISSN: 2597-9914

Jurnal Kimia Sains dan Aplikasi 28 (8) (2025): 405-415

Jurnal Kimia Sains dan Aplikasi
Journal of Scientific and Applied Chemistry

Journal homepage: http://ejournal.undip.ac.id/index.php/ksa

Synthesis and Characterization of Palm Shell Activated Carbon for Adsorption of Remazol Brilliant Violet 5R

Walny Nicha [1], Mohammad Wijaya M. [1,*], Hasri [1]

[1] Department of Chemistry, Faculty of Mathematics and Natural Sciences, Universitas Negeri Makassar, Makassar, Indonesia

* Corresponding author: wijasumi@unm.ac.id

https://doi.org/10.14710/jksa.28.8.405-415

Article Info

Article history:

Received: 14th March 2025
Revised: 19th August 2025
Accepted: 19th August 2025
Online: 31st October 2025

Keywords:
Palm Shell; Activated carbon; Remazol Brilliant Violet; Adsorption

Abstract

This study aims to characterize activated carbon derived from palm kernel shells treated with 10% H_3PO_4 and evaluate its effectiveness as an adsorbent for removing Remazol Brilliant Violet 5R (RBV5R) dye. The adsorption capacity of the activated carbon was assessed based on adsorption efficiency using a batch adsorption method. The experimental process included preparation, carbonization, chemical activation, characterization, and adsorption studies conducted using a continuous system. Scanning Electron Microscopy (SEM) analysis of the unactivated carbon revealed that the pores were partially obstructed by residual carbonized substances, resulting in narrower pore structures. In contrast, activation with 10% H_3PO_4 produced larger and cleaner pores due to the effective removal of surface residues. Fourier-transform infrared spectroscopy (FTIR) analysis of the raw carbon identified functional groups such as O–H, C=C, and C– H, while the activated carbon exhibited characteristic peaks corresponding to C=O, P–O, and P–OH groups. Surface area analysis indicated a significant increase from 2202.532 m^2/g for the unactivated carbon to 5137.431 m^2/g after activation. Adsorption studies demonstrated that both adsorbents achieved optimal dye removal performance at pH 3 and a contact time of 20 minutes. The unactivated carbon achieved an adsorption efficiency of 84.618% and an adsorption capacity of 6.346 mg/g, while the activated carbon exhibited identical efficiency and capacity values.

1. Introduction

The development of the batik industry in Indonesia to meet the community's clothing needs has expanded beyond Java and is now growing in South Sulawesi, particularly in Makassar. In 2020, the number of batik industries in Indonesia was estimated to reach 6,120 units, with a production value of approximately 4.89 trillion rupiah per year [1]. The batik industry in Makassar has also played a pioneering role in expanding batik business units across the country. While the growth of the batik industry has had positive economic and cultural impacts, the waste generated from the batik dyeing process poses significant environmental concerns [2].

The batik production process consumes a significant amount of water and chemicals, particularly synthetic dyes such as Remazol, Indigosol, and Naphthol. During the fabric dyeing process, only about 5% of the dye is absorbed by the fabric, while the remaining 95% is discharged as liquid waste [3]. In Makassar's batik industry, Remazol-type synthetic dyes, including Remazol Brilliant Violet-5R (RBV5R), are commonly used. Based on its structure, RBV5R is a reactive dye from the azo group (-N=N) with a chromophore group, enabling it to produce bright, long-lasting colors on fabric fibers, making it a popular choice in the batik industry [4]. However, RBV5R structure contains C=O and -C=C bond groups, making it highly resistant to degradation (Figure 1). When released into aquatic environments, this dye can contaminate water sources used for human consumption, potentially causing health issues such as skin, eye, respiratory, and digestive irritation. Additionally, prolonged exposure to RBV5R has been linked to an increased risk of cancer.

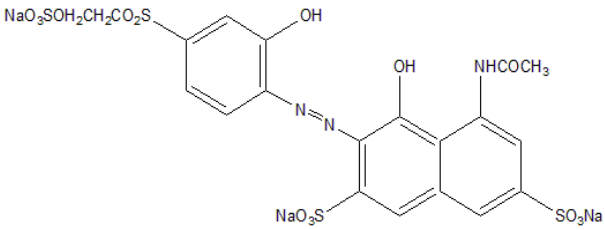

Figure 1. Structure of Remazol Brilliant Violet-5R (RBV5R)) [5]

Various alternatives to reduce synthetic dye pollution are coagulation, oxidation, degradation, ion exchange, biological, and adsorption methods [5]. The adsorption method is considered one of the most favorable techniques due to its high efficiency, large adsorption capacity, and low operational cost [6]. Adsorption is when a substance (molecule or ion) is absorbed onto the surface of the adsorbent pores [7]. Generally, adsorption processes are classified into two types: batch and continuous methods. In the batch method, a specific amount of adsorbent is mixed with a fixed volume of solution, and the change in solute concentration is monitored over a certain time interval. In contrast, the continuous method maintains constant contact between the adsorbent and the solution, allowing adsorption to proceed until the adsorbent reaches saturation [8]. Common commercial adsorbents include zeolite, silica gel, alumina, and activated carbon.

Activated carbon is a widely used adsorbent due to its highly porous structure. Additionally, it has a larger surface area than other adsorbents, allowing it to adsorb greater substances [9]. A wide range of raw materials can be utilized to produce activated carbon, including wood, sawdust, seed husks, rice husks, shells, peat, bagasse, coal, lignite, and animal bones [10]. Chemically activated carbon exhibits a higher adsorption capacity than non-activated carbon. Research on different carbon activators, $ZnCl_2$, KOH, and H_3PO_4, demonstrated iodine adsorption capacities of 552.015 mg/g, 621.81 mg/g, and 767 mg/g, respectively, with phosphoric acid-activated carbon exhibiting the highest iodine adsorption [11]. The activation process using phosphoric acid enhances pore formation and increases the number of cavities on the carbon surface, thereby improving its adsorption capacity [12].

According to data from the North Luwu Agriculture Office of South Sulawesi Province, the area of oil palm plantations increased to 23,988.42 hectares in 2021, yielding 386,174.60 tons of oil palm [13]. The processing of every ton of oil palm generates approximately 6.5% (65 kg) of palm kernel shell waste, making proper utilization essential to create valuable products and reduce environmental pollution. Oil palm shells contain 44% lignin, 27.7% cellulose, and 21.6% hemicellulose [14]. Due to their high lignin content, oil palm shells serve as a suitable raw material for producing activated carbon.

Activated carbon produced from oil palm empty fruit bunches and activated with H_3PO_4 has demonstrated an adsorption efficiency of 87.23% and a maximum adsorption capacity of 3.0373 mg/g for remazol dye [15]. H_3PO_4-activated carbon has also been reported to possess a moisture content of 2.81%, an ash content of 3.68%, and an iodine adsorption capacity of 344.22% [16]. Therefore, in this study, activated carbon derived from phosphoric acid-activated palm shells is utilized as an adsorbent to reduce the concentration of RBV5R dye. The study aims to investigate the effects of contact time and pH on the adsorption process of RBV5R dye using palm shell-based activated carbon under batch adsorption conditions.

2. Experimental

2.1. Materials and Instruments

The materials used in this study included oil palm shells, H_3PO_4 (Merck, 85%), NaOH (PA, 99%), HCl 0.5 M and 1 M (Merck, 37%), CH_3COOH (PA, 99.8%), CH_3COONa (Merck, 99%), KH_2PO_4 (Merck, 99%), K_2HPO_4 (Merck, 98%), Na_2HPO_4 (Merck, 99%), NH_4Cl (PA, 99.5%), RBV5R dye, and aluminum foil. The equipment used comprised glassware, a mortar and pestle, a spatula, a pH meter, a shaker, an oven, a furnace, an analytical balance, a 100-mesh sieve, a desiccator, a centrifuge, glass bottles, reagent bottles, a Scanning Electron Microscope (SEM, JEOL JSM 6063LA), a Fourier Transform Infrared Spectrometer (FTIR, Prestige-21), a Surface Area Analyzer (SAA, Quantachrome Touchwin v1.22), and an Ultraviolet-Visible Spectrophotometer (UV-Vis, Labomed Auto UV 2602).

2.2. Preparation of Palm Kernel Shell (PKS) Activated Carbon

The palm kernel shells (PKS) were thoroughly washed with running water to remove impurities and then sun-dried to eliminate surface moisture. The dried shells were crushed into pieces measuring approximately 1-2 cm. The crushed shells were subjected to preliminary thermal treatment for 30 minutes to produce palm shell carbon, followed by carbonization at 650°C for 2 hours [17]. The carbonization process aimed to increase the surface area of the carbon by decomposing the organic components and releasing combustible gases such as CO, CH_4, H_2, formaldehyde, methane, formic acid, and acetic acid, along with unburned substances like CO_2, H_2O, and liquid tar [18].

After carbonization, the carbon was crushed and sieved to achieve a uniform size, maximizing activation efficiency. The pores on the carbon's surface were initially covered by residual carbonization byproducts; therefore, activation was performed using a 10% H_3PO_4 solution to remove these residues, enhance the surface area, and improve adsorption capacity [19]. The carbon was then immersed in a 10% H_3PO_4 solution, stirred for 1 hour, and left to stand for 24 hours. The activated carbon was then washed with distilled water to remove any remaining impurities and neutralize its pH. Finally, the carbon was dried in an oven at 105°C and allowed to cool to room temperature.

2.3. PKS Activated Carbon Characterization

The adsorbents (unactivated carbon and activated carbon) were characterized using SEM to analyze their surface morphology, FTIR to identify functional groups, and SAA to determine their specific surface area.

2.4. Preparation of RBV5R Solution

A total of 0.50 g of RBV5R dye powder was dissolved in distilled water in a 500 mL volumetric flask to prepare a 1000 ppm stock solution. A 50 ppm RBV5R solution was then prepared by diluting the 1000 ppm stock solution.

2.5. Determination of Maximum Wavelength of RBV5R

The 50 ppm RBV5R solution was analyzed using a UV-Vis spectrophotometer within a wavelength range of 400–800 nm to determine its maximum absorption [6].

2.6. Standard Solution Curve Preparation

RBV5R solutions with concentrations of 10, 20, 30, 40, and 50 ppm were analyzed using a UV-Vis spectrophotometer at the wavelength of maximum absorption. The absorbance values were recorded to generate a calibration curve, representing the correlation between RBV5R concentration and absorbance [15].

2.7. Adsorption Process

2.7.1. Determination of Optimum Contact Time

A total of 0.1 g of adsorbent was placed into a 250 mL Erlenmeyer flask containing 15 mL of 50 ppm RBV5R solution. A concentration of 50 ppm was selected because lower concentrations enable more accurate monitoring of adsorption or degradation processes, particularly when using UV–Vis spectrophotometry. At higher or too low concentrations, absorbance values may exceed the linear range of the spectrophotometer, leading to less reliable data due to signal saturation or deviation from the Beer–Lambert law [20, 21]. The flask was then placed on a shaker at 150 rpm with varying contact times of 20, 40, 60, 80, and 100 minutes [6]. After the adsorption process, the solution was centrifuged at 3000 rpm for 30 minutes. The resulting filtrate was analyzed using a UV-Vis spectrophotometer, and the adsorption efficiency was calculated using Equations 1 and 2 [22].

2.7.2. Determination of Optimum Sample Solution pH

RBV5R solutions with a concentration of 50 ppm at pH values of 3, 5, 7, 9, and 11 were prepared from a 1000 ppm stock solution. A total of 10 mL of the stock solution was transferred into a 400 mL beaker. A digital pH meter was inserted, and the pH was adjusted using 0.5 M HCl for acidic conditions and 1 M NaOH for basic conditions [16]. Once the desired pH was achieved, the solution was transferred to a 200 mL graduated cylinder, followed by the addition of the appropriate buffer solution to maintain the pH value. After that, a total of 0.1 g of adsorbent was placed into a 250 mL Erlenmeyer flask containing 15 mL of 50 ppm RBV5R solution with pH variations of 3, 5, 7, 9, and 11 [23]. The Erlenmeyer flask was covered with aluminum foil and placed on a shaker at 150 rpm for the previously determined optimum contact time. After adsorption, the solution was centrifuged at 3000 rpm for 30 minutes. The resulting filtrate was analyzed using a UV-Vis spectrophotometer, and adsorption efficiency was calculated using Equations 1 and 2.

$$Adsorption\ capacity\ (Q) = \frac{(C_0 - C_e)V}{m} \quad (1)$$

$$Adsorption\ efficiency\ (\%) = \frac{(C_0 - C_e)}{C_0} \times 100\% \quad (2)$$

Where C_0 is the concentration before the adsorption process, C_e is the concentration after the adsorption process, V is the volume of the solution, and m is the mass of the adsorbent.

3. Results and Discussion

3.1. PKS Activated Carbon Characterization

3.1.1. SEM Analysis

Characterization using SEM aims to analyze the surface morphology of unactivated carbon and activated carbon. As shown in Figure 2a, the SEM analysis of unactivated carbon reveals the presence of pores; however, these pores are partially blocked by residual carbonization byproducts, leading to a narrowed surface area. To address this, the carbon undergoes activation through immersion in a phosphoric acid solution, which helps remove or decompose the remaining carbonized substances.

The activation process enhances porosity by breaking hydrocarbon bonds and oxidizing surface molecules, resulting in pore enlargement and an overall increase in surface area [12]. The SEM results of activated carbon treated with H_3PO_4 10%, shown in Figure 2b, confirm this effect. The image illustrates a more porous structure with significantly reduced impurities, demonstrating the effectiveness of the activation process. The greater the number of pores formed, the larger the surface area, which improves the adsorption capacity of activated carbon.

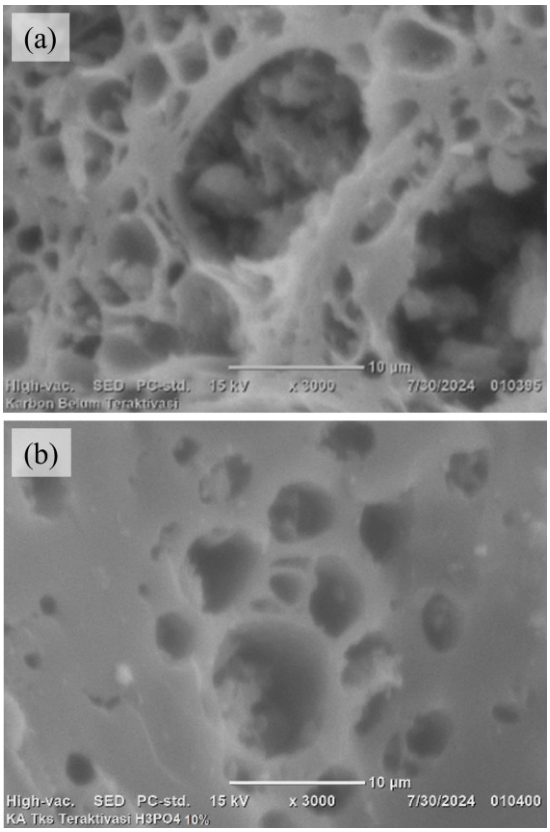

Figure 2. Surface morphology of a) unactivated carbon and b) activated carbon at 3000× magnifications

3.1.2. FTIR Analysis

Characterization using FTIR aims to identify functional groups and bond types found in unactivated carbon and activated carbon. As shown in Figure 3 presents the FTIR spectra of unactivated carbon and activated carbon with phosphoric acid. The FTIR analysis of unactivated palm shell carbon indicates the presence of O-H functional groups at a wavenumber of 3444.87 cm^{-1}. Vibrations at 1622.16 cm^{-1} correspond to C=O groups with low intensity, while peaks at 2924.09 cm^{-1} and 2374.37 cm^{-1} represent C-H bonds from hemicellulose. Additionally, a peak at 1556.20 cm^{-1} signifies aromatic C=C bonds from lignin.

After activation with 10% H_3PO_4, notable spectral changes occur, including peak shifts, intensity reductions, and the emergence of new peaks. The O-H functional group shifts to 3408.22 cm^{-1}, while the C-H peak at 2376.30 cm^{-1} decreases in intensity. The C=O group at 1622.13 cm^{-1} exhibits higher intensity, indicating successful activation, as C=O functional groups are characteristic of activated carbon [24]. Additionally, the C=C bond from lignin appears at 1558.48 cm^{-1}, while a peak at 1082.07 cm^{-1} corresponds to the C-O bond in activated carbon. The presence of P-O and P-OH functional groups at 956.69 cm^{-1} confirms the influence of phosphoric acid activation [25].

The disappearance of the C-H group and the increased intensity of the C=O peak in activated carbon suggest the removal of impurities, leading to a more reactive carbon surface [12]. Phosphoric acid activation enhances the polarity of the resulting activated carbon, as indicated by the dominance of O-H, C-O, and C=O functional groups [24].

3.1.3. SAA Analysis

Characterization using SAA was conducted to determine the surface area, pore volume, and pore size distribution of unactivated carbon and activated carbon. The BET results (Figure 4) show the adsorption–desorption isotherms of carbon and activated carbon, illustrating the relationship between nitrogen gas volume and pressure. The amount of adsorbed gas is measured by increasing the gas pressure and recording the uptake from a known gas volume. The isotherms of both samples do not conform to the IUPAC classification of adsorption isotherms, and no hysteresis loop is observed, making it impossible to estimate the pore characteristics of the adsorbents.

Based on Figures 5a and 5b, the pore size distribution of unactivated carbon shows a maximum adsorption value of 1.1996 cc/nm/g at a radius of 1.0854 nm and a maximum desorption value of 1.1732 cc/nm/g at a radius of 1.0958 nm, resulting in a pore size range of 1.09–1.19 nm. In contrast, activated carbon exhibits a maximum adsorption value of 2.6452 cc/nm/g at a radius of 1.2114 nm and a maximum desorption value of 2.7040 cc/nm/g at a radius of 1.1018 nm, corresponding to a pore size range of 1.10–1.21 nm. A comparison of the specific surface areas (SAA) from BET and BJH analyses is summarized in Table 1.

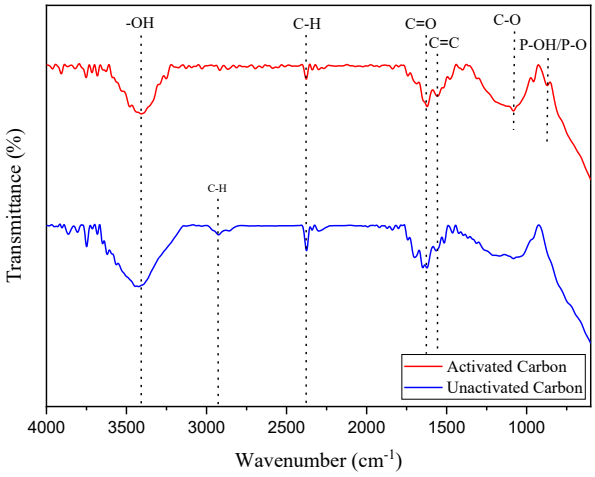

Figure 3. FTIR spectra of unactivated carbon and activated carbon

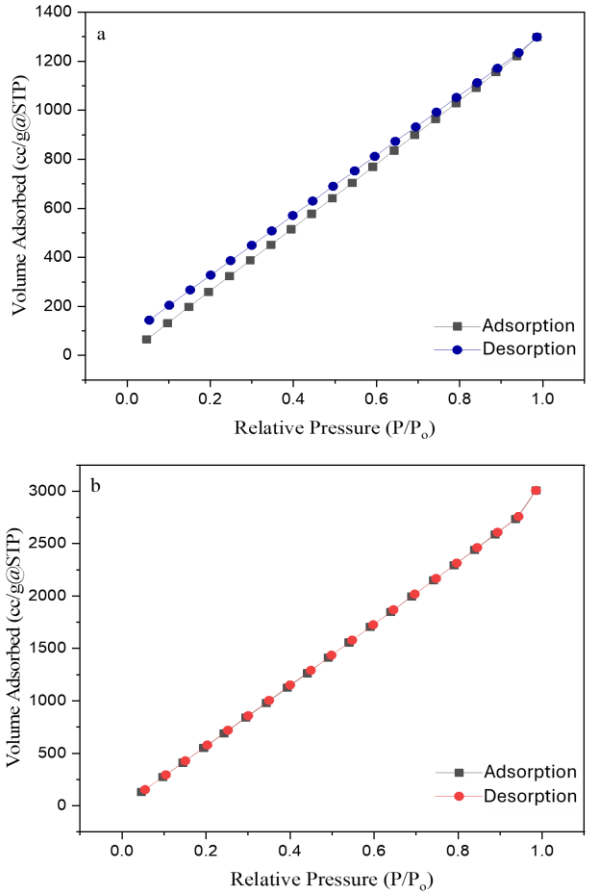

Figure 4. N_2 adsorption-desorption isotherm graphs of (a) unactivated carbon and (b) activated carbon

Table 1 shows that the results of SAA characterization of activated carbon using H_3PO_4 has a surface area of 5137.431 m^2/g with a pore volume measuring 6.18075 cc/g and an average pore diameter of 1.21136 nm, while the carbon that does not undergo activation with H_3PO_4 solution has a surface area of 2202.532 m^2/g with a pore volume measuring 2.69962 cc/g and an average pore diameter of 1.08542 nm. This shows that activated carbon has a better surface area and pore volume to be used as an adsorbent than unactivated carbon.

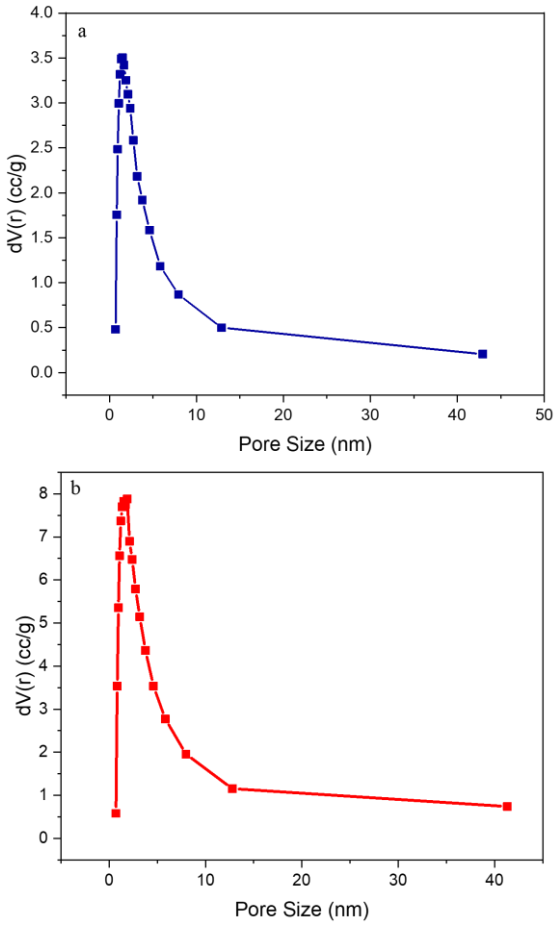

Figure 5. BJH adsorption pore size distribution curve of (a) unactivated carbon and (b) activated carbon

Table 1. Results of SAA analysis of unactivated and activated carbon

Characteristic	Unactivated Carbon	Activated carbon
Surface area (m^2/g)	2202.532	5137.431
Pore volume (cc/g)	2.69962	6.18075
Pore diameter (nm)	1.08542	1.21136

The larger the surface area of an adsorbent, the greater its adsorption capacity. A high surface area and pore volume of activated carbon enhance its adsorption efficiency, allowing more adsorbate to be absorbed by the adsorbent [26]. The use of H_3PO_4 solution as an activating agent also influences the surface area, as this strong acid can remove hydrocarbon compounds or impurities, thereby promoting pore formation on the carbon surface. The adsorption capacity of activated carbon increases with the concentration of the activating agent [6].

3.2. Determination of Optimum Wavelength of RBV5R

Determination of the optimum wavelength was carried out to determine the wavelength that gave maximum absorption to the analyte, which was characterized by the highest absorbance value of the RBV5R solution. Determination of the optimum wavelength was carried out using a UV-Vis spectrophotometer in the wavelength range of 400-650 nm for a 50 ppm RBV5R solution. The optimum wavelength of the RBV5R solution is shown in Figure 6.

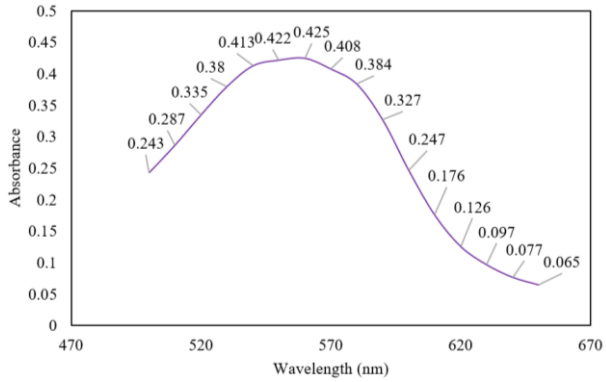

Figure 6. The optimum wavelength of RBV5R

Based on Figure 6, the optimum wavelength of the RBV5R solution was determined to be 560 nm, corresponding to the highest absorbance value of 0.425 among the measured wavelengths. This result is consistent with the findings of [27], which reported a maximum wavelength of 559 nm for the RBV5R solution. Therefore, the wavelength of 560 nm was selected for absorbance measurements in the batch adsorption experiments.

3.3. Results of the Batch Adsorption Method

3.3.1. Optimum Time of Unactivated and Activated Carbon

The determination of the optimum contact time was conducted to identify the most effective duration for the adsorption of RBV5R dye using activated carbon. Contact time is an important parameter in evaluating the adsorption performance of an adsorbent. As contact time increases, the concentration of RBV5R dye in the solution decreases, while the adsorption efficiency correspondingly increases [28]. The batch adsorption experiments for both unactivated and activated carbon were carried out with contact time variations of 20, 40, 60, 80, and 100 minutes.

Figure 7 shows that contact time variation during the batch adsorption process significantly affected the amount of dye adsorbed onto both unactivated and activated carbon surfaces. At a contact time of 20 minutes, unactivated carbon showed an average adsorption efficiency of 6.45%, an adsorption capacity of 0.484 mg/g, and a final dye concentration of 46.78 ppm. In comparison, adsorption using activated carbon achieved a much higher average efficiency of 40.51%, with an adsorption capacity of 3.04 mg/g and a final dye concentration of 29.74 ppm. These results indicate that the active sites on the activated carbon surface interacted more effectively with dye molecules than those on unactivated carbon, leading to higher adsorption efficiency and capacity. However, beyond 40 minutes, the adsorption process tended to stabilize, suggesting that the adsorbent surface had become saturated and equilibrium was established between the dye molecules and the adsorbent. Prolonged contact time may even result in partial desorption of dye molecules from the adsorbent surface [10]. The possible adsorption mechanism between activated carbon and RBV5R dye is illustrated in Figure 8.

Table 2. Data from the determination of the optimum contact time using unactivated carbon

t (minute)	C_0 (ppm)	Abs	C_t (ppm)	%E (%)	Q (mg/g)	$\bar{C}_t$	$\overline{\%E}$	$\bar{Q}$	STD
20		0.405	46.8171	6.366	0.477				
		0.401	46.3293	7.341	0.551	46.776	6.447	0.484	0.857
		0.408	47.1829	5.634	0.423				
40		0.413	47.7927	4.415	0.331				
		0.418	48.4024	3.195	0.240	48.240	3.520	0.264	0.784
		0.419	48.5244	2.951	0.221				
60		0.416	48.1585	3.683	0.276				
	50	0.423	49.0122	1.976	0.148	48.524	2.951	0.221	0.879
		0.418	48.4024	3.195	0.240				
80		0.421	48.7683	2.463	0.185				
		0.422	48.8902	2.220	0.166	48.646	2.707	0.203	0.645
		0.417	48.2805	3.439	0.258				
100		0.422	48.8902	2.220	0.166				
		0.425	49.2561	1.488	0.112	48.931	2.138	0.160	0.614
		0.420	48.6463	2.707	0.203				

Table 3. Data from the determination of the optimum contact time using activated carbon

t (minute)	C_0 (ppm)	Abs	C_t (ppm)	%E (%)	Q (mg/g)	$\bar{C}_t$	$\overline{\%E}$	$\bar{Q}$	STD
20		0.267	29.988	40.024	3.002				
		0.269	30.232	39.537	2.965	29.744	40.512	3.038	1.291
		0.259	29.012	41.976	3.148				
40		0.283	31.939	36.122	2.709				
		0.294	33.28	33.439	2.508	32.589	34.821	2.612	1.343
		0.288	32.549	34.902	2.618				
60	50	0.288	32.549	34.902	2.618				
		0.296	33.524	32.951	2.471	33.402	33.195	2.490	1.599
		0.301	34.134	31.732	2.380				
80		0.301	34.134	31.732	2.380				
		0.308	34.988	30.024	2.252	34.907	30.187	2.264	1.470
		0.313	35.598	28.805	2.160				
100		0.316	35.963	28.073	2.105	35.476	29.049	2.179	0.879

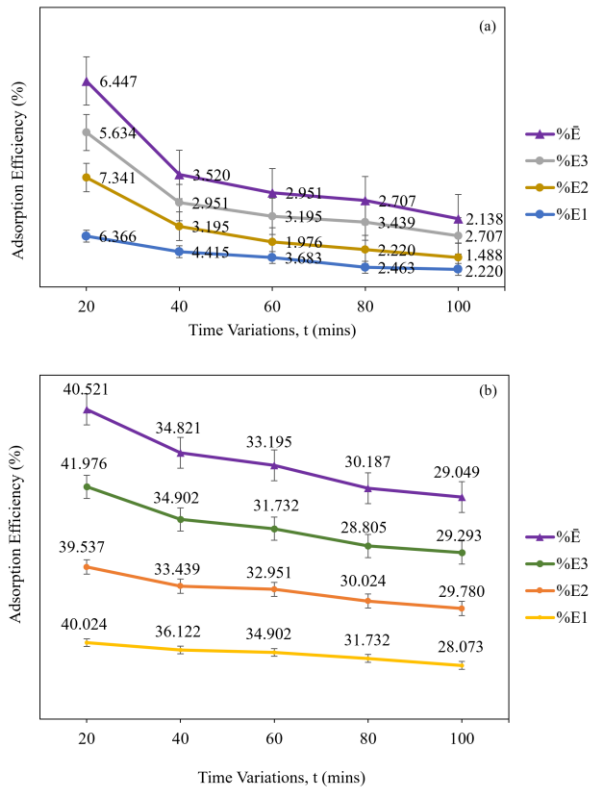

Figure 7. Adsorption efficiency of RBV5R using (a) unactivated and (b) activated carbon at different times

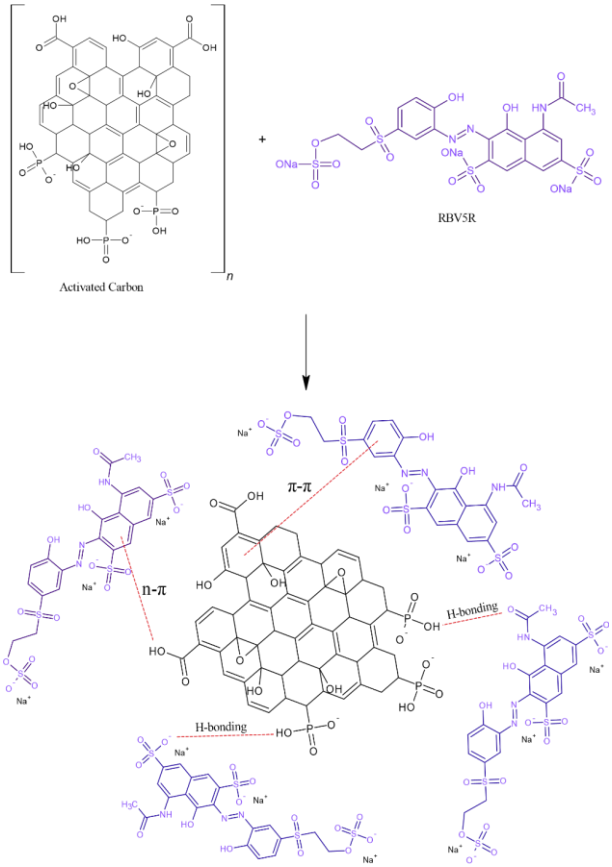

Figure 8. Illustration of possible interaction mechanisms between activated carbon and RBV5R dye [29, 30]

3.3.2. Optimum pH of Unactivated and Activated Carbon

The optimum pH of the solution is determined to identify the most favorable conditions, either acidic or alkaline, for the adsorption of RBV5R dye by unactivated and activated carbon. pH is a critical parameter, as excessively low or high pH levels can significantly influence the adsorption performance of the adsorbent. The interaction between activated carbon and RBV5R dye is likely facilitated by hydrogen bonding, which plays a key role in the adsorption mechanism [16]. In this study, the optimum pH was determined by evaluating the adsorption performance at various pH levels of 3, 5, 7, 9, and 12.

As shown in Figure 9, the increasing pH of the solution significantly affects the amount of dye adsorbed on the surface of the activated carbon. The results indicate that a more acidic pH enhances both adsorption efficiency and adsorption capacity, whereas a more alkaline pH leads to a decrease in both parameters. At pH 3, unactivated carbon showed its highest efficiency (8.233%), adsorption capacity (0.617 mg/g), and final dye concentration (45.88 ppm). Activated carbon achieved much higher values, with 84.618% efficiency, 6.346 mg/g capacity, and 7.691 ppm final concentration. These results suggest that adsorption is most effective at low pH, where the abundant H^+ ions protonate the activated carbon surface, generating positively charged sites that attract the negatively charged RBV5R dye molecules through electrostatic interaction [28].

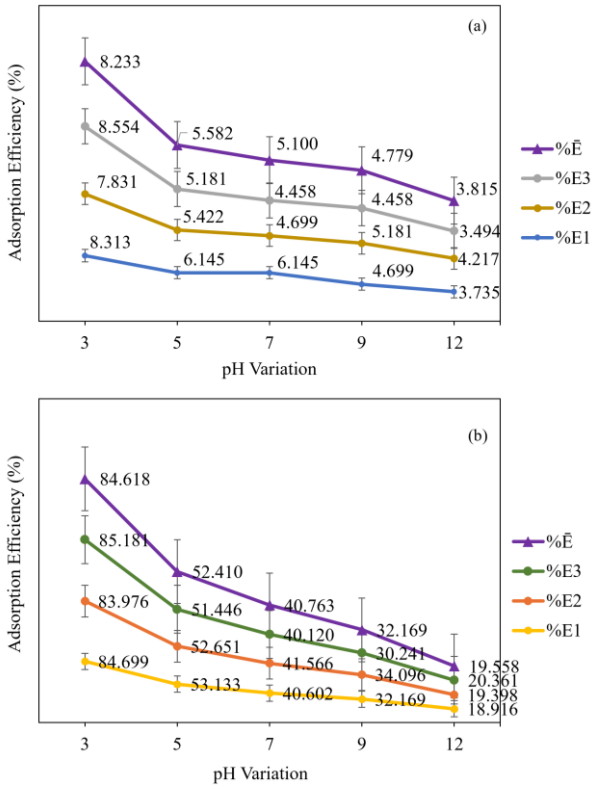

Figure 9. Adsorption efficiency of RBV5R using (a) unactivated and (b) activated carbon at different pH values

Table 4. Determination of the optimum pH of the solution using unactivated carbon

t (min)	C_o (ppm)	pH	Abs	C_t (ppm)	%E (%)	Q_t (mg/g)	$\overline{C_t}$	$\overline{\%E}$	$\overline{Q_t}$	STD
		3	0.403	45.843	8.313	0.623				
			0.405	46.084	7.831	0.587	45.884	8.233	0.617	0.368
			0.402	45.723	8.554	0.642				
		5	0.412	46.928	6.145	0.461				
			0.415	47.289	5.422	0.407	47.209	5.582	0.419	0.502
			0.416	47.410	5.181	0.389				
		7	0.412	46.928	6.145	0.461				
20	50		0.418	47.651	4.699	0.352	47.450	5.100	0.383	0.912
			0.419	47.771	4.458	0.334				
		9	0.418	47.651	4.699	0.352				
			0.416	47.410	5.181	0.389	47.610	4.779	0.358	0.368
			0.419	47.771	4.458	0.334				
		12	0.422	48.133	3.735	0.280				
			0.420	47.892	4.217	0.316	48.092	3.815	0.286	00368
			0.423	48.253	3.494	0.262				

At pH 5, a decrease in adsorption efficiency was observed, which may be attributed to the lower concentration of H^+ ions compared to pH 3. As a result, the electrostatic attraction between the adsorbent and the adsorbate was weaker [23]. From pH 7 to pH 12, both adsorption efficiency and adsorption capacity continued to decline. This is likely due to an increase in OH^- ions in the RBV5R solution, which occupies the active sites of the adsorbent and causes deprotonation, leading to increased electrostatic repulsion between the negatively charged adsorbent and dye molecules [31, 32]. At pH 12, the color of the RBV5R solution changes from dark violet to light violet, which may result from the deprotonation of functional groups and the breakdown of azo (-N=N-) and sulfonate ($-SO_3^-$) groups due to hydrolysis by hydroxide ions (OH^-) [33, 34].

3.4. Comparison Study of Activated Carbon from Palm Shells with Other Reported Adsorbents on RBV5 Adsorption

In this study, the adsorption performance of RBV5R onto activated carbon was compared with previously reported adsorbents. As shown in Table 6, the adsorption of RBV5R using activated carbon derived from palm shells exhibited superior performance compared to other reported adsorbents, achieving the highest adsorption efficiency of 84.618%. This indicates that the developed activated carbon possesses promising characteristics and is effective for treating colorant-containing wastewater. Overall, the RBV5R adsorption capacity of activated carbon derived from coconut shells showed lower uptake compared to that of palm shell-based activated carbon developed in this study, whereas graphene oxide and green marine algae exhibited higher uptake capacities.

Table 5. Data from the determination of the optimum pH solution using activated carbon

t (min)	C_0 (ppm)	pH	Abs	C_t (ppm)	%E (%)	Q_t (mg/g)	$\overline{C_t}$	$\overline{\%E}$	$\overline{Q_t}$	STD
		3	0.086	7.651	84.699	6.352				
			0.089	8.012	83.976	6.298	7.691	84.618	6.346	0.606
			0.084	7.410	85.181	6.389				
		5	0.217	23.434	53.133	3.985				
			0.219	23.675	52.651	3.949	23.795	52.410	3.931	0.869
			0.224	24.277	51.446	3.858				
		7	0.269	29.699	40.602	3.045				
20	50		0.265	29.217	41.566	3.117	29.618	40.763	3.057	0.736
			0.271	29.940	40.120	3.009				
		9	0.304	33.916	32.169	2.413				
			0.296	32.952	34.096	2.557	33.916	32.169	2.413	1.928
			0.312	34.880	30.241	2.268				
		12	0.359	40.542	18.916	1.419				
			0.357	40.301	19.398	1.455	40.221	19.558	1.467	0.736
			0.353	39.819	20.361	1.527				

Table 6. Comparison of palm shell–based activated carbon with previously reported adsorbents

Clasiffication	This study	Hidayati *et al.* [4]	Yuliani *et al.* [35]	Bello and Ahmad [36]	Gokulan *et al.* [37]
Adsorbent type	Activated carbon from palm shells	Coconut shells	Graphene Oxide	Activated carbon from periwinkle shells	Green marine algae
Surface area (m^2/g)	5137.431	-	-	1894.0	-
Adsorption capacity (mg/g)	6.346	1.4377	65.03	-	159.7
Adsorption efficiency (%)	84.618	75.59	67.3	81.28	81.2

4. Conclusion

Activated carbon synthesized from palm kernel shell (PKS) demonstrated high effectiveness in the adsorption of RBV5R dye. SEM analysis of the unactivated carbon revealed that the pores were covered with residual carbonized substances, resulting in narrower pore structures. In contrast, activation using 10% H_3PO_4 produced carbon with larger and cleaner pores, indicating the successful removal of carbonaceous residues from the surface. FTIR analysis of the unactivated carbon identified the presence of O–H, C=O, C=C, and C–H functional groups, while the activated carbon exhibited characteristic peaks corresponding to P–O and P–OH groups at a wavenumber of 956.69 cm^{-1}, confirming successful activation. Surface area analysis showed a substantial increase from 2202.532 m^2/g for unactivated carbon to 5137.431 m^2/g for activated carbon. Adsorption of Remazol Brilliant Violet 5R (RBV5R) using both adsorbents reached optimal performance at pH 3 and a contact time of 20 minutes. The activated carbon achieved an adsorption efficiency of 84.618% and an adsorption capacity of 6.346 mg/g, demonstrating its superior performance compared to unactivated carbon.

Acknowledgment

The author would like to express sincere gratitude to all parties who contributed to the success of this research, particularly Dr. Mohammad Wijaya M, S.Si., M.Si., for his financial support. The author also gratefully acknowledges the support of Universitas Negeri Makassar for this research.

References

[1] Siregar Abi Pratiwa, Raya Alia Bihrajihant, Nugroho Agus Dwi, Indana Fairuz, I. Made Yogya Prasada, Andiani Riesma, Simbolon Theresia Gracia Yunindi, Kinasih Agustina Tri, Upaya Pengembangan Industri Batik di Indonesia, *Dinamika Kerajinan dan Batik*, 37, 1, (2020),

[2] Fitriyah Fitriyah, Tauny Akbari, Irfan Alfandiana, Pengolahan Limbah Cair Batik Banten secara Koagulasi Menggunakan Tawas dan Adsorpsi dengan Memanfaatkan Zeolit Alam Bayah, *Jurnal Serambi Engineering*, 7, 1, (2022), 2499-2509

[3] Herfiani Zikrina Hanifah, Rezagama Arya, Nur Muhammad, Pengolahan Limbah Cair Zat Warna Jenis *Indigosol Blue* (*C.i Vat Blue 4*) Sebagai Hasil Produksi Kain Batik Menggunakan Metode Ozonasi

dan Adsorpsi Arang Aktif Batok Kelapa Terhadap Parameter COD dan Warna, *Jurnal Teknik Lingkungan*, 6, 3, (2017), 1-10

[4] Puspita Hidayati, Ita Ulfin, Hendro Juwono, Adsorpsi zat warna *remazol brilliant blue R* menggunakan *nata de coco*: optimasi dosis adsorben dan waktu kontak, *Jurnal Sains dan Seni ITS*, 5, 2, (2016),

[5] Hong Jian Lai, Adsorption of Remazol Brilliant Violet 5R (RBV-5R) and Remazol Brilliant Blue R (RBBR) from Aqueous Solution by Using Agriculture Waste, *Tropical Aquatic and Soil Pollution*, 1, 1, (2021), 11-23 https://doi.org/10.53623/tasp.v1i1.10

[6] Siswanti Siswanti, Afifah Hasna Oktafiana, Yobellya Putri, Adsorpsi Zat Warna *Remazol Brilliant Blue R* pada Limbah Industri Batik Menggunakan Adsorben dari Mahkota Buah Nanas, *Eksergi*, 21, 1, (2023), 9-16 https://doi.org/10.31315/e.v21i1.10669

[7] Imam Fathoni, Rusmini, Pemanfaatan Bentonit Teknis Sebagai Adsorben Zat Warna, *UNESA Journal of Chemistry*, 5, 3, (2016), 18-22

[8] Sella August Putri, A. Asnawati, Dwi Indarti, Optimalisasi Adsorpsi Zat Warna Rhodamin B pada Hemiselulosa dalam Sistem Dinamis, *Berkala Sainstek*, 7, 1, (2019), 1-6 https://doi.org/10.19184/bst.v7i1.9681

[9] Amelina Dwika Hardi, Rahma Joni, Syukri Syukri, Hermansyah Aziz, Pembuatan Karbon Aktif dari Tandan Kosong Kelapa Sawit sebagai Elektroda Superkapasitor, *Jurnal Fisika Unand*, 9, 4, (2021), 479-486

[10] Syarifuddin Oko, Harjanto Harjanto, Andri Kurniawan, Cici Winanti, Penurunan Kadar Zat Warna *Remazol Brilliant Blue R* dengan Metode Adsorpsi Menggunakan Serbuk $CaCO_3$ dari Cangkang Telur dan Karbon Aktif, *METANA*, 18, 1, (2022), 39-45 https://doi.org/10.14710/metana.v18i1.45766

[11] Marina Olivia Esterlita, Netti Herlina, Pengaruh penambahan aktivator $ZnCl_2$, KOH, dan H_3PO_4 dalam pembuatan karbon aktif dari pelepah aren (*Arenga pinnata*), *Jurnal Teknik Kimia USU*, 4, 1, (2015), 47-52 https://doi.org/10.32734/jtk.v4i1.1460

[12] Vidyanova Anggun Mentari, Gewa Handika, Seri Maulina, Perbandingan gugus fungsi dan morfologi permukaan karbon aktif dari pelepah kelapa sawit menggunakan aktivator asam fosfat (H_3PO_4) dan asam nitrat (HNO_3), *Jurnal Teknik Kimia USU*, 7, 1, (2018), 16-20 https://doi.org/10.32734/jtk.v7i1.1629

[13] The Center for International Forestry Research and World Agroforestry (CIFOR-ICRAF), in: Landscape Design Document North Luwu, 2021, https://darikebunkelanskapsehat.id/lokasi-penelitian/luwu-utara/

[14] Hani Alfiyani, Nurlina Nurlina, Nelly Wahyuni, Adsorpsi Anilin oleh Karbon Aktif Magnetik Cangkang Kelapa Sawit, *ALCHEMY Jurnal Penelitian Kimia*, 18, 2, (2022), 130-139 https://dx.doi.org/10.20961/alchemy.18.2.53647.130-139

[15] Denny Aris Setiawan, Sirajuddin, Wanwol Ricky Marthin De Tulus, Adsorption of Remazol Brilliant Blue R Dye Using Activated Carbon from Emty Palm Oil Bunches, *Sains Natural: Journal of Biology and Chemistry*, 13, 4, (2023), 183-190 https://doi.org/10.31938/jsn.v13i4.527

[16] Anita Imawati, Adhitiyawarman, Kapasitas Adsorpsi Maksimum Ion Pb (II) oleh Arang Aktif Ampas Kopi Teraktivasi HCl dan H_3PO_4, *Jurnal Kimia Khatulistiwa*, 4, 2, (2015), 50-61

[17] Hanna Najmia, Emmy Sri Mahreda, Rizqi Putri Mahyudin, Kissinger Kissinger, Pemanfaatan Arang Aktif Cangkang Kelapa Sawit Teraktivasi H_3PO_4 untuk Penurunan Kadar Besi (Fe), Mangan (Mn) dan Kondisi pH pada Air Asam Tambang, *EnviroScienteae*, 17, 1, (2021), 30-37 https://dx.doi.org/10.20527/es.v17i1.11351

[18] Alieftiyani Paramita Gobel, A Taufik Arief, Pengaruh Karbonisasi Terhadap Karakteristik Tempurung Kelapa Berdasarkan Uji Proksimat Dan Nilai Kalor, *Jurnal Mineral, Energi, dan Lingkungan*, 5, 1, (2021), 48-54 https://doi.org/10.31315/jmel.v5i1.5370

[19] Sahara Hamas Intifadhah, Rahmawati Munir, Dadan Hamdani, Adrianus Inu Natalisanto, Suhadi Muliyono, Surface Area Analysis of Activated Carbon Material From Palm Frond Waste using Different Activation Agents, *Indonesian Journal of Applied Physics*, 15, 1, (2025), 193-203 https://doi.org/10.13057/ijap.v15i1.96045

[20] Asep Bayu Dani Nandiyanto, Risti Ragadhita, Muhammad Aziz, How to Calculate and Measure Solution Concentration using UV-Vis Spectrum Analysis: Supporting Measurement in the Chemical Decomposition, Photocatalysis, Phytoremediation, and Adsorption Process, *Indonesian Journal of Science and Technology*, 8, 2, (2022), 345-362

[21] Orla P. Murphy, Mayank Vashishtha, Parimaladevi Palanisamy, K. Vasanth Kumar, A Review on the Adsorption Isotherms and Design Calculations for the Optimization of Adsorbent Mass and Contact Time, *ACS Omega*, 8, 20, (2023), 17407-17430 https://doi.org/10.1021/acsomega.2c08155

[22] Thamrin Azis, La Ode Ahmad, Keke Awaliyah, Laode Abdul Kadir, Study of Kinetics and Adsorption Isotherm of Methylene Blue Dye using Tannin Gel from *Ceriops tagal*, *Jurnal Kimia Sains dan Aplikasi*, 23, 10, (2020), 370-376 https://doi.org/10.14710/jksa.23.10.370-376

[23] Indah Riwayati, Ni'matul Fikriyyah, Suwardiyono, Adsorpsi Zat Warna *Methylene Blue* Menggunakan Abu Alang-Alang (*Imperata cylindrica*) Teraktivasi Asam Sulfat, *Jurnal Inovasi Teknik Kimia*, 4, 2, (2019), 6-11 https://doi.org/10.31942/inteka.v4i2.3016

[24] Rosliana Eso, Luvi, Ririn, Efek Variasi Konsentrasi Zat Aktivator H_3PO_4 Terhadap Morfologi Permukaan dan Gugus Fungsi Karbon Aktif Cangkang Kemiri, *Gravitasi*, 20, 1, (2021), 19-23

[25] S. M. Yakout, G. Sharaf El-Deen, Characterization of activated carbon prepared by phosphoric acid activation of olive stones, *Arabian Journal of Chemistry*, 9, (2016), S1155-S1162 https://doi.org/10.1016/j.arabjc.2011.12.002

[26] Diharyo, Salampak, Zafrullah Damanik, Sulmin Gumiri, Pengaruh Lama Aktifasi dengan H_3PO_4 dan Ukuran Butir Arang Cangkang Kelapa Sawit Terhadap Ukuran Pori dan Luas Permukaan Butir Arang Aktif, *Prosiding Seminar Nasional Lingkungan Lahan Basah*, 2020

[27] Suseno Suseno, Petrus Darmawan, Peni Pujiastuti, Sumardiyono Sumardiyono, Degradation Degradasi Pewarna Tekstil Remazol Violet 5R dengan Metode

Elektrooksidasi Menggunakan Elektroda Grafit, *Jurnal Sains Teknologi dan Lingkungan*, 8, 2, (2022), 204-210 https://doi.org/10.29303/jstl.v8i2.370

[28] Mesy Cintia, Ni Luh Gede Ratna Juliasih, Dian Herasari, Agung Abadi Kiswandono, R. Supriyanto, Studi Karbon Aktif Kayu Bakau (*Rhizophora Mucronata*) Sebagai Adsorben Pewarna Tekstil Biru Tua Kode 5 Menggunakan Spektrofotometer UV-Vis, *Analit: Analytical and Environmental Chemistry*, 7, 1, (2022), 54-67

[29] Azduwin Khasri, Mohd Ridzuan Mohd Jamir, Anis Atikah Ahmad, Mohd Azmier Ahmad, Adsorption of Remazol Brilliant Violet 5R dye from aqueous solution onto melunak and rubberwood sawdust based activated carbon: interaction mechanism, isotherm, kinetic and thermodynamic properties, *Desalination and Water Treatment*, 216, (2021), 401-411 https://doi.org/10.5004/dwt.2021.26852

[30] Sumiati Side, Diana Eka Pratiwi, Nita Magfirah Ilyas, Mega Putri Aulia Rahim, Suriati Eka Putri, Pengaruh Aktivasi Terhadap Morfologi Karbon Aktif dari Kulit Kacang Tanah, *Indonesian Journal of Fundamental Sciences*, 9, 2, (2023), 111-117 https://doi.org/10.26858/ijfs.v9i2.54397

[31] Rahmiana Zein, Indah Tika Marliani, Emriadi Emriadi, Putri Ramadhani, Syiffa Fauzia, Potensi Biosorben Kulit Batang Sagu (*Metroxylon sago*) untuk Penyerapan Zat Warna *Crystal Violet*: Studi Isoterm, Kinetika, Termodinamika, dan Aplikasi, *Journal of The Indonesian Society of Integrated Chemistry*, 15, 2, (2023), 83-98 https://doi.org/10.22437/jisic.v15i2.29245

[32] Ariyanto Eko, Lestari Dian Dwi, Kharismadewi Dian, Analisa Kemampuan dan Kinetika Adsorpsi Karbon Aktif dari Cangkang Ketapang terhadap Zat Warna Metil Oranye, *Jurnal Dinamika Penelitian Industri*, 32, 2, (2021), 166-178

[33] S. Fatimah, W. Wiharto, R. Fatoni, Electrodecolorization of remazol violet with graphite electrodes : Application Of Statistical Designs And Regression Analysis, *IOP Conference Series: Materials Science and Engineering*, 620, 1, (2019), 012016 https://doi.org/10.1088/1757-899X/620/1/012016

[34] Vanessa Jane Zainip, Liyana Amalina Adnan, Mohamed Soliman Elshikh, Decolorization of Remazol Brilliant Violet 5R and Procion Red MX-5B by Trichoderma Species, *Tropical Aquatic and Soil Pollution*, 1, 2, (2021), 108-117 https://doi.org/10.53623/tasp.v1i2.25

[35] Dilla Dwi Yuliani, F. Fitrilawati, Norman Syakir, Pengaruh pH pada Efisiensi Adsorpsi dan Kapasitas dalam Proses Adsorpsi *Rhodamine B* oleh *Graphene Oxide*, *Jurnal Material dan Energi Indonesia*, 14, 2, (2024), 84-91 https://doi.org/10.24198/jme.v14i2.53131

[36] Olugbenga Solomon Bello, Mohd Azmier Ahmad, Removal of Remazol Brilliant Violet-5R dye using periwinkle shells, *Chemistry and Ecology*, 27, 5, (2011), 481-492 https://doi.org/10.1080/02757540.2011.600696

[37] R. Gokulan, A. Avinash, G. Ganesh Prabhu, J. Jegan, Remediation of remazol dyes by biochar derived from *Caulerpa scalpelliformis*—An eco-friendly approach, *Journal of Environmental Chemical Engineering*, 7, 5, (2019), 103297 https://doi.org/10.1016/j.jece.2019.103297